water

MDPI

Article

Trace Metals and Metalloids Present in Springwater of a Mining Area: Assessment Based on Chemical and Isotopic Data (δ^2H, $\delta^{18}O$, ^3H and $^{87}Sr/^{86}Sr$)

José Alfredo Flores Ronces [1], Edith R. Salcedo Sánchez [2,*], Manuel Martínez Morales [3], Juan Manuel Esquivel Martínez [2], Oscar Talavera Mendoza [4] and María Vicenta Esteller Alberich [5]

1 Maestría en Recursos Naturales y Ecología, Universidad Autónoma de Guerrero, Acapulco de Juárez 39390, Mexico; ron_alf23@hotmail.com
2 Consejo Nacional de Ciencia y Tecnología-Escuela Superior de Ciencias de la Tierra, Universidad Autónoma de Guerrero, Taxco el Viejo 40323, Mexico; jmesquivel@conacyt.mx
3 Instituto Mexicano de Tecnología del Agua, Jiutepec 62550, Mexico; manuelm@tlaloc.imta.mx
4 Escuela Superior de Ciencias de la Tierra, Universidad Autónoma de Guerrero, Taxco el Viejo 40323, Mexico; otalavera.uagro@gmail.com
5 Instituto Interamericano de Tecnología y Ciencias del Agua (IITCA), Universidad Autónoma del Estado de México, Toluca 50120, Mexico; mvestellera@uaemex.mx
* Correspondence: ersalcedo@conacyt.mx or edithsalcedos@gmail.com

Abstract: The Taxco mining district is a well-known international producer of silver, jewelry, and precious metal handicrafts. Inappropriate disposal wastes from anthropogenic activities have been deteriorating the hydric resources and threatening the inhabitants' health, since they use the springwater for human consumption and domestic activities. A multi-tracer approach combining measurements of hydrochemical data, trace elements, and isotopes δ^2H, $\delta^{18}O$, ^3H, and $^{87}Sr/^{86}Sr$ ratios was undertaken for 18 springwater samples. $\delta^{18}O$ and δ^2H indicate that the springwater comes from the rain and had experienced some degree of isotopic fractionation by atmospheric evaporation in some samples at lower altitudes. ^3H values on the springwater showed the existence of old and new water. Three groups of springwater were identified according to age: local flow in rhyolites, intermediate flow through red beds to the outcrop point in sandstone and shales, and deep flow in greenschist. The results of this study show the utility of $^{87}Sr/^{86}Sr$ ratios in identifying the water–rock interactions and springwater flow paths, suggesting that more widespread use of the strontium isotopic fingerprint is warranted.

Keywords: springwater; water isotopes; water rock interactions; $^{87}Sr/^{86}Sr$ ratio; mixing processes

check for updates

Citation: Flores Ronces, J.A.; Sánchez, E.R.S.; Martínez Morales, M.; Esquivel Martínez, J.M.; Talavera Mendoza, O.; Esteller Alberich, M.V. Trace Metals and Metalloids Present in Springwater of a Mining Area: Assessment Based on Chemical and Isotopic Data (δ^2H, $\delta^{18}O$, ^3H and $^{87}Sr/^{86}Sr$). *Water* **2023**, *15*, 1917. https://doi.org/10.3390/w15101917

Academic Editor: Elias Dimitriou

Received: 31 March 2023
Revised: 12 May 2023
Accepted: 16 May 2023
Published: 18 May 2023

1. Introduction

The study of water resources in mining areas is very important because of the increasing demand for and pollution and depletion of groundwater [1–3]. Groundwater is an important component of the hydrological cycle, and even more so in recharge areas of the regional aquifers, and in some cases, as a source of water for human consumption [4–6]. Springwater represents an important source of drinking water in many countries around the world, where the importance of water quality in human health has recently attracted a great deal of interest [7]. Springwater is fundamental to rural communities since it is the main source of water, given that these communities are usually located in regions with complex stakeholder relationships [8].

Several studies have shown that springwater is one of the environmental areas most threatened by urbanization processes and mining activity; these threats to aquifers become evident with reduced or eliminated recharge areas and the detriment of water quality [4,7,8]. Understanding the hydrogeological functioning of a region is fundamental; the knowledge of groundwater dynamics, including potential recharge elevations, flow directions, and the recognition of natural and anthropic hydrogeochemical impacts, is imperative to enhance the protection and management of springwater resources [9,10].

Isotopic composition in springwater has been recognized by its application in understanding hydrological systems, sources of water, recharge elevations, residence time, and solutes and identifying geochemical reactions [1–6,9] and the release and transport of toxic elements, which provides information on the dispersion and management of groundwater resources [11–13]. The isotopes of hydrogen (δ^2H) and tritium ($\delta^{\delta 3}$H), oxygen (oxygen-18 or δ^{18}O), and the ratio of strontium-87 to strontium-86 (^{87}Sr/^{86}Sr) have long been used in hydrology [9,11,12]. Their application as powerful natural tracers allows groundwater evolution to be studied in hydrogeological problems [13–17]. The stable oxygen and hydrogen isotopes are environmental isotopes that exist ubiquitously in natural waters; the stable isotopes of δ^{18}O and δ^2H in water have long been used in hydrology for investigating water composition and circulation in the whole water cycle; the isotopic compositions in water are affected by meteorological process (e.g., temperature, humidity, etc.) and geographical factors (latitude, longitude, and altitude) and, to a lesser extent, by reactions with geologic material, making them suitable for investigating groundwater provenance. Hence, these isotopes are useful fingerprints of groundwater and tracers of groundwater mixing and recharge processes [12–15]. Strontium isotopes are also good tracers for water–rock interaction studies. Oxygen, deuterium, and strontium isotopes occur naturally, but tritium concentrations increased abruptly following atmospheric testing of H-bombs during the 1950s and 1960s [17]. Tritium is a natural radioactive isotope of hydrogen and part of the water molecule; its concentration can be used to determine the residence times in the hydrologic system. Detectable concentrations of this isotope in groundwater provide evidence that recharge has occurred after nuclear bomb tests [3,14,18]. The groundwater obtains dissolved Sr from the recharge areas (infiltration processes), and along its flow path, through dissolution or ion exchange with minerals. Therefore, ^{87}Sr/^{86}Sr ratios give insight into water–rock interaction processes and determine the origin, transit time, flow patterns, regimes of water, geological structure, hydrogeochemical, and hydrogeologic processes that involve mixing of waters of different chemical and/or isotopic compositions [12,16,19].

Taxco has been a famous silver producer since pre-Hispanic times, and it was one of the richest silver mines in the world and important in the national and international trade of jewelry and the manufacturing of handcrafts. For decades, these activities in the area generated large amounts of tailings wastes, which were deposited in dumps around the city; mining activities in the region terminated in early 2009 due to the depletion of ore reserves, a decrease in the market price of silver, and labor disputes [20,21]. Furthermore, this area is part of the aquifer recharge zone, in addition to the fact that the springs are one of the main sources of water supply for the city [22,23]. Because of the lack of good-quality surface water reservoirs owing to the harsh pollution conditions, springwater constitutes the most widely available source of fresh water [24,25].

Several studies have indicated that the waters of the San Juan Taxco system represent a health risk for the inhabitants and the biota due to the high concentrations of potentially toxic elements, due to their persistence, permanence, and bioaccumulation in aquatic organisms, causing serious damage to aquatic organisms and human health through the food chain and water resources [20,24,25].

The general purpose of this study is to explain the processes controlling springwater quality and chemical changes produced by water–rock interactions in a mining area, based on chemical and isotopic data. According to this general objective, the following will also be studied: (1) the origin of the water springs, (2) the influence of water–rock interactions on the origin of trace metals and metalloids, and (3) water quality for drinking purposes. This study will contribute to establishing foundation data for future water supply assessment and management, and this information is crucial to understanding the mobilization of constituents of geological materials.

2. Materials and Methods

2.1. Study Area

Taxco mining region is located in the southern part of the Mexican Republic, in the north of the State of Guerrero, at 1778 masl (meters above sea level) and with an extension of about 750 km^2. The study area is located between the parallels 18°27′ and 18°34′ and the meridians 99°39′ and 99°34′ West of Greenwich (Figure 1). It includes the Taxco town and neighboring localities.

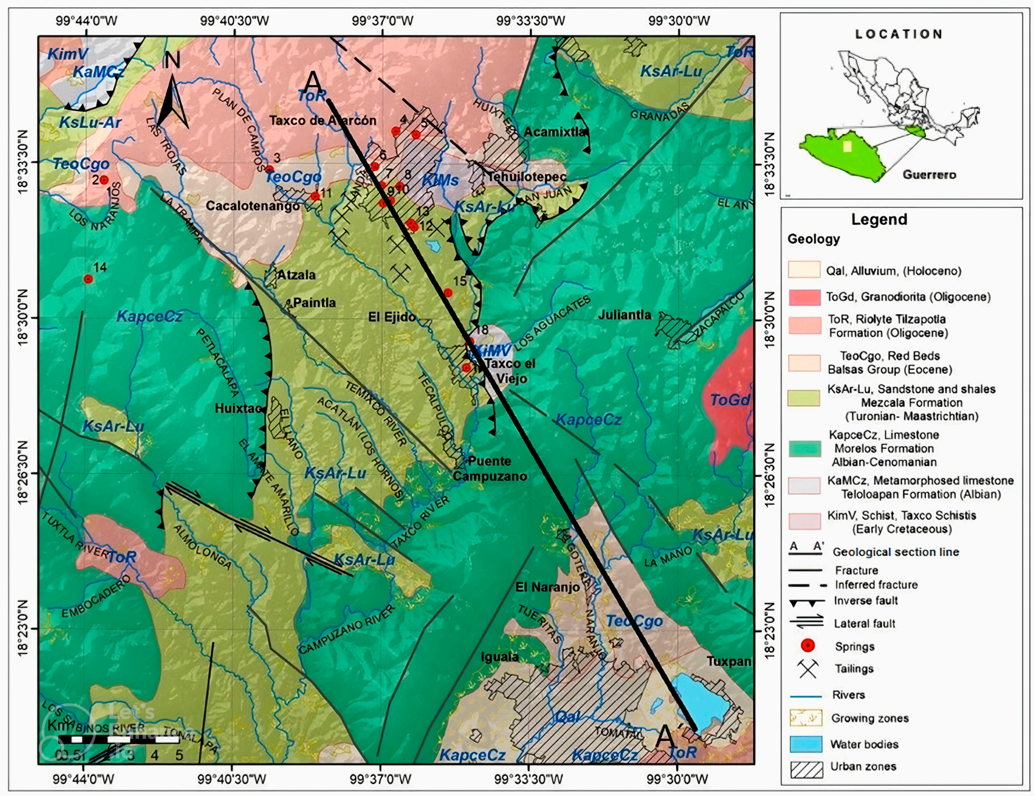

Figure 1. Location of the study area sampled springs and geological map of Taxco, Guerrero.

The Köppen Climate Classification is "Cwb" oceanic subtropical highland. The annual mean temperature in Taxco is 21.9 °C, and the warmest month is April, with a mean temperature of 24 °C. The coolest month is December, with a mean of 20 °C. The annual mean of precipitation is 1214 mm, the rainiest month is September with 254 mm, and the driest month is February with 7.6 mm (1980–2020) [24,26].

The Taxco mining district is famous worldwide for its history of extraction and exploitation of minerals that dates back to pre-Hispanic times. Modern mining in Taxco began in the 1940s, coming from the exploitation of Ag-Cu-Pb-Zn and precious metals (Ag, Au) using the selective flotation method, which substantially increased the capacity of production [21,27]. Intensive mining produced large quantities of liquid and solid mining wastes containing toxic metals [21]. The solid wastes were deposited in mill tailings dams, accounting for more than 55 million tons of unoxidized and oxidized mining wastes accumulating in six major impoundments around Taxco (Figure 1) and making the water of the area susceptible to pollution from trace metals and metalloids [21,28,29].

Tailings have been characterized as containing PTE such as lead, barium, cadmium, zinc, iron, arsenic, strontium, and sulfur in high concentrations and minerals such as quartz, feldspars, ferromagnesians (pyroxene, amphibole), carbonates (calcite, rhodochrosite, siderite), and sulfates (barite, gypsum). Hypogenic sulfides include pyrite, pyrrothite, marcasite, galena, sphalerite, and chalcopyrite. Secondary minerals are abundant and include smithsonite, gypsum, clay minerals, jarosite, beudantite, hematite, magnetite, bernalite, chalcocite, and a selection of soluble sulfates such as hexahydrite, basanite, pickeringite, and epsomite [21,25,28].

Several investigations in the study area have documented the negative impact on surface water, stream sediments, and soils; these studies indicate that around 10.000 ha of soil around the mining tailings have concentrations of toxic elements above the regional background levels and that both wild and crop vegetation show a severe impact by toxic elements [21,24,25,28–31]. Some health risks were detected in women of reproductive age by exposure to multiple sources of lead around the El Fraile tailings [20,32].

2.2. Geological and Hydrogeological Setting

The geological map of the Taxco region shows the lithology and location of tailing impoundments (Figure 1). The rocks in the study area consist of Lower Cretaceous metamorphic rocks of the Taxco Schist Formation, Albian-Cenomanian limestone of the Morelos Formation, Upper Cretaceous sandstone and shale of the Mexcala Formation, Lower Tertiary red beds or detrital materials of continental origin of the Balsas Group, and Middle Tertiary acidic volcanic rocks of the Tilzapotla Formation [33]. Mineralized structures in the study area are represented by hydrothermal veins, replacing structures and stockworks hosted in limestone and more rarely in schists and red beds. Vein trends range from both N to S and NW to SE, coinciding with major regional structures [33]. Mineralized structures are 1–3 m in width (although a few reaches 10 m) and 700–2000 m in length (Figure 2).

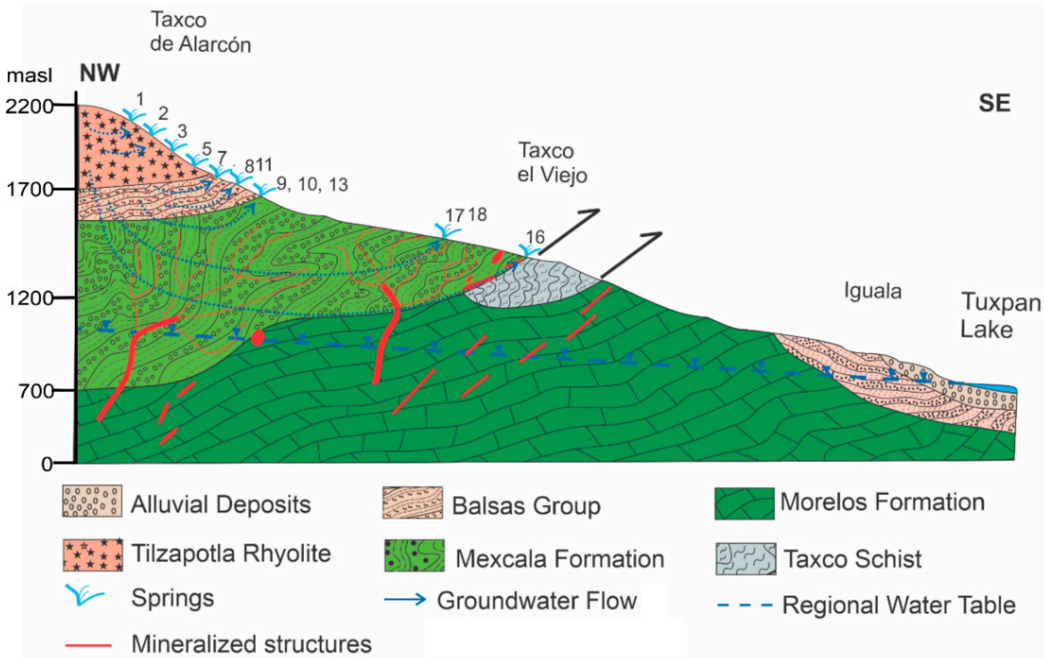

Figure 2. Geological cross-section.

The study area includes a portion of the recharge zone of a regional aquifer (administratively called the Buenavista-Iguala aquifer); this territory has been partially banned from groundwater exploitation by Mexican laws since 1978 [22,23]. The recharge zone is located in a mountainous region with a rugged topography that does not allow the development of conventional water supply sources (wells and dams); therefore, the population uses surface runoff and springs that are distributed throughout the region for drinking water, domestic consumption, and livestock.

The springs under this study had their origin in rainwater that infiltrates into the upper portion of the watershed in the unsaturated zone (Figure 2). Once the rainwater is incorporated into the ground, it flows through the different geological materials along its flowpath. The uppermost formation is made up of rhyolitic volcanic rocks; therefore, the groundwater mainly moves through the fractures that have been developed in the geological material or the porosity of volcanoclastic horizons. In this context, the springs outflow at different altitudes, depending on the geometry of the structures.

As mentioned before, the area where the springs are located belongs to the recharge zone, and no boreholes have been drilled, since the depth to the regional water table has been estimated to be at least 1100 masl [22,23]. No hard data about the water table elevation of the regional aquifer are available for the recharge zone, and only conceptual models have been developed for this region, proposing rainwater flowing from the upper elevations through faults and fractures and finally feeding the exploitable aquifers at lower elevations.

In the regional aquifer, the hydrogeological units are composed of rhyolites from the Tilzapotla Formation, gravels and sandstones from the Balsas Group, shales from Mexcala Formation and finally limestones from the Morelos Formation. On the other hand, the storage section of the groundwater is made up of the alluvial and fluvial sediments (clay, silt, sand, and gravels) that are restricted to the channels of the streams, as well as in the alluvial sediments and tuffs of lower areas (in the Iguala Valley). The geological section (Figure 2) has two aquifers: (1) an upper unconfined aquifer and (2) a lower confined aquifer. The upper aquifer gradually thickens towards the center of the lower elevation areas (valleys), reaching up several hundred meters [22,23]. The lower aquifer is housed in a sequence of marine sedimentary rocks, represented by the limestones and sandstones of the Morelos and Mexcala Formations, respectively (Figure 2). These two aquifers are separated by confining and semi-confining rocks consisting of shales and siltstones from the Balsas Group. The hydrogeological basement is represented by Taxco Schist, made up of metamorphic rocks [22]. The groundwater discharges in the lower parts of the region. Some portion of the groundwater drains into the main streams, and the remaining portion discharges as a groundwater flow to the Tuxpan Lake [23].

2.3. Sample Collection and Analyses

To obtain detailed information about groundwater, a water-sampling campaign of springs was conducted in February 2017, collecting in situ data of physicochemical parameters and carrying out chemical analyses of the main components, namely stable and radiogenic isotopes. The sampling was carried out during the dry season to avoid alterations to the geochemistry of the water, since the rainy season is accompanied by the dragging of suspended material and landslides in the study area.

Eighteen springwater samples for drinking use were collected according to the protocols explained in norm NOM-230-SSA1-2002 [34] in compliance with APHA, AWW, and WEF guidelines [35]. To determine field parameters, a conductivity meter, pH electrode, and ORP probe were used to read water temperature, electrical conductivity (EC), and redox potential (Eh) with a Hanna meter. TDS was calculated based on the electrical conductivity of the solution in the multiparametric Hanna meter. The concentrations of springwater samples were measured in the Geochemistry Laboratory at the Autonomous University of Guerrero, and the cation samples were filtered using 0.40–0.45 µm nitrocellulose membrane (Millipore, 0.45 µm mesh), acidified to pH < 2 with HNO_3 at the time of collection, and stored at a temperature of 4 °C. The anion samples were filtered through 0.40–0.45 µm nitrocellulose membrane without acidification. Alkalinity and chloride contents were determined by titration with 0.02M HCl and 0.01M $AgNO_3$, respectively (all titrations were performed in duplicate). Bicarbonate ions ($HCO_3{}^-$) were calculated using the following formula [36]:

$$HCO_3^-\left(mgL^{-1}\right) = \frac{Alcalinity\ \ (mgL^{-1})}{\left(1+\frac{2+10-10.3}{10^{-pH}}\right)*50}*61$$

Sulfates, nitrates, and fluorine contents were measured using a Hach DR890 colorimeter with a precision and accuracy of ±0.300 and 0.208, ±0.500 and 0.184, and ±0.035 and 0.060 mg L^{-1}, respectively, using a SulfaVer (sulfate) and NitraVer (nitrate) powder packet as standard at 25 and 50 mg L^{-1}, respectively, and SPADNS reagent as a standard of

1.00 mg L^{-1} for fluorides. Concentrations of the other ions were measured by Inductively coupled plasma-atomic emission spectra (ICP-AES) in a PerkinElmer Optima 3200 DV instrument (PerkinElmer, Foster City, Calif.). The detection limits (mg L^{-1}) during the measurements were Mg (0.03), Ca (0.0067), K (0.1468), Fe (0.0007), Ba (0.0007), Cu (0.0006), Zn (0.0008), As (0.0087), SiO_2 (0.0053), Cr (0.0022), and Pb (0.0038). Sodium was measured using a flame atomic absorption spectrophotometer (FAAS) in a PerkinElmer Analyst 100 instrument. The precision and accuracy were determined using High-Purity Certified Standards of Wastewater (CWW-TM-D; CWWTMH; CWW-TM-A, and CWW-TM-E).

Five springwater samples were taken for the study of δ^2H and $\delta^{18}O$, and eleven samples for ^3H; the analyses were conducted in the laboratory of Isotopic Hydrology at the Mexican Institute of Water Technology by Laser Absorption Spectroscopy technique using a Cavity Ringdown Spectrometer model L2110-i Picarro for δ^2H and $\delta^{18}O$ and a Liquid Scintillation Spectrometer model Quantulus GCT 6220 following the protocols of the International Atomic Energy Agency (IAEA) and National Institute of Standards and Technology for ^3H. The error associated with the oxygen was ± 0.05 and ± 0.1 for deuterium; the tritium measurements correspond to 1σ, and the detection limit of the used methodology was 0.6 UT. Fourteen strontium isotope analyses of samples were conducted in the Laboratory of Geochemistry of the Department of Geosciences at University of Arizona. $^{87}Sr/^{86}Sr$ ratios were measured by Thermal Ionization Mass Spectrometry in a VGA Instrument following the protocol defined by Thibodeau et al. [37]. The analytical reproducibility was checked by analyzing the NBS-987 standard which gave $^{87}Sr/^{86}Sr = 0.710260 \pm 0.000013$ (n = 54.1 σ).

Water quality was evaluated according to criteria established for human consumption by the World Health Organization [38] and by Mexican standards NOM-127-SSA1-1994 [39]. Finally, the data were statistically analyzed, and the charge balance error factor of the springwater samples was found to be within an acceptable range from 0.24% to 5.20% (the results were summarized in Table 1). In addition, the Piper diagram was developed to define the different hydrochemical facies using Geochemist's Workbench (GWB) [40].

The recharge altitudes were determined by applying stable isotope contents $\delta^{18}O$ or δH^2. The altitude effect is most often expressed as an isotopic lapse rate and given as a per mil change in $\delta^{18}O$ of precipitation per 100 m of elevation change. In this case, the relationship between $\delta^{18}O$ and altitude was determined by direct measurements in the National Isotopic Network of Mexico (IMTA), considering those stations in Morelos and Guerrero States.

Table 1. Physical and chemical characteristics of springwater samples (TDS: total dissolved solids, <dl: detection limit; <ql: quantification limit).

Limits/Spring ID	pH	EC	Eh	TDS	Total Hardness $CaCO_3$	HCO_3^-	NO_3^-	SO_4^{2-}	Cl^-	Na^{2+}	Mg^{2+}	Ca^{2+}	K^+	Fe^{2+}	Mn^{2+}	Ba	Cu^{2+}	Zn^{2+}	As	SiO_2	F^-	Pb
	Units	(μS/cm)	(mV)	(mgL^{-1})																		
NOM-SSA1-127-2021	**6.5–8.5**	**-**	**-**	**1000**	**500**		**11**	**400**			**-**	**-**		**0.3**	**0.15**	**1.3**	**2**	**5**	**0.025**	**-**	**1.5**	**0.01**
WHO, 2017		**-**	**-**	**1000**	**100**		**40**	**250**						**0.1**	**0.4**	**0.7**	**1**	**5**	**0.01**	**-**	**1.5**	
Horconcito 1	6.56	44.6	201.72	41.5	11.2	24.8	1.35	1	<dl	5.91	2.91	3.46	2.91	0.05	<dl	0.05	<ql	<ql	<ql	20.25	<ql	<ql
Horconcito 2	6.76	41.7	224.23	38.6	12.7	24.0	2.01	<dl	<dl	4.16	0.38	3.52	2.86	0.04	<ql	<ql	<ql	<ql	<ql	24.1	<ql	<ql
Cascada	6.9	35.9	171.42	32.3	12.9	20.0	1.64	<dl	<dl	3.78	0.44	3.62	3.12	0.26	<ql	0.03	<ql	<ql	<ql	14.8	0.04	<ql
Chacoalco	6.83	89.6	263.95	83.6	27.7	52.0	0.94	1	0.83	7.3	3	9.84	2.18	<ql	<ql	<ql	<ql	<ql	<ql	34.87	0.08	<ql
Mulata	5.61	113.6	277.3	g	32.5	42.0	14.78	10	8.33	23.67	0.73	9	3.2	0.08	<ql	0.03	<ql	<ql	<ql	29.25	0.08	<ql
Pozitos	7.46	730.7	175.19	609.1	404.9	258.0	6.16	104	25	13.17	20.88	130.5	1.8	0.07	0.291	0.2	<ql	0.041	<ql	19.64	0.2	<ql
Landa	6.7	681.4	181.98	694.4	297.1	389.7	13.19	104	35.83	11.29	20	77	0.52	0.03	<ql	0.11	<ql	<ql	<ql	12.22	0.44	<ql
Pedro Martin	7.28	404.9	193.81	295.9	155.1	102.0	6.3	61	33.33	26.9	6.13	52.04	3.77	0.16	<ql	0.05	<ql	<ql	0.015	14.99	0.3	<ql
Cacalotenango	7.1	529.7	227.16	498	288	300.0	4.04	17	7.5	9.8	6.57	101.6	0.98	<ql	<ql	0.09	<ql	<ql	<ql	19.29	0.41	<ql
Ejido Arroyo 1	6.72	609.4	197.14	589.2	377.9	328.0	11.97	63	3.3	11.27	12.27	143.2	0.81	0.16	<ql	0.04	<ql	<ql	<ql	11.03	0.34	<ql
Ejido Arroyo 2	6.83	645.8	118.35	622.5	391.8	342.0	8.59	69	2.83	8.96	1.38	160	8.91	0.3	<ql	<ql	<ql	<ql	<ql	10.92	0.27	0.018
Arroyo 1	7.04	661.1	197.02	565.9	377.5	248.0	14.14	100	17.5	6.73	8.04	146	0.64	0.08	0.041	<ql	<ql	<ql	<ql	9.71	0.44	<ql
Arroyo 2	7.2	563.3	149.4	483	270.4	216.0	1.5	88	15.83	26.27	6.46	110	1.68	0.09	0.042	<ql	<ql	<ql	<ql	10.12	0.34	<ql
Atzala	7.87	379.6	208.88	322.9	203.9	182.0	1.6	7	10.83	4.45	2.47	80.21	0.67	<ql	<ql	0.04	<ql	<ql	<ql	12.02	0.03	<ql
Taxco el Viejo 1	6.68	953.9	240.77	839	583.4	358.0	47.3	130	57	16.67	14.25	222.3	1.61	0.05	<ql	0.12	<ql	<ql	<ql	12.02	0.4	0.012
Taxco el Viejo 2	6.85	941.3	210.53	814.5	516.2	288.0	5.25	230	35	36.02	30.01	172.7	2.54	0.05	0.133	0.11	<ql	<ql	<ql	9.84	0.63	0.012
Huamuchilito	7.06	361.5	119.51	328.7	164.7	184.0	1.48	30	<dl	16.8	4.37	69.44	5.03	0.7	1.1	1.12	<ql	<ql	<ql	21.06	0.36	<ql
Hueymatla	7.01	593.1	99.44	564.8	340.9	320.0	1.79	51	<dl	10.59	8.59	140	1.77	0.13	0.036	0.07	<ql	<ql	<ql	9.91	0.33	<ql

3. Results and Discussion

3.1. Main Hydrochemical Features

The Piper diagram shows the main hydrogeochemical features grounded on the relative dominance of major cations and anions in terms of their reacting values, as well as their spatial evolution (Figure 3). Three types of hydrochemical facies were identified in the Taxco region: Group 1, sodic bicarbonate water (HCO_3–Na), includes five samples with a high sodium and low chlorine content (springs Horconcito 1 and 2, Cascada, Chacualco, and Mulata). The Na+ and HCO_3- enrichment due to rainwater and weathering of plagioclase in the highest part of the region.

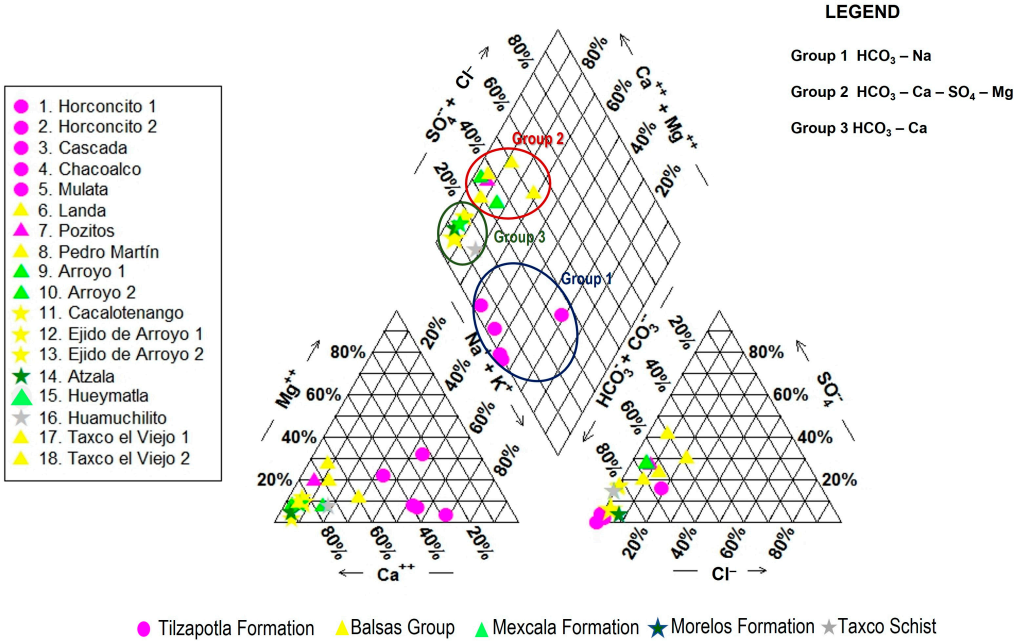

Figure 3. Piper diagram of hydrochemical data in the study area.

Group 2, calcium bicarbonate water, has a low to medium sulfate and magnesium content (HCO_3–Ca–SO_4–Mg) and is composed of seven springs (Landa, Pozitos, Pedro Martín, Arroyo 1 and 2, Taxco el Viejo 1 and 2); this group shows enrichment in HCO_3–Ca–SO_4–Mg due to the flow of springwater through carbonate material. UIt presents high contents of Ca^{2+} and Mg^{2+}, released during the interaction of water with carbonates from limestones. The sulfate content is related to anthropogenic activities and the lixiviation of tailings.

Group 3, calcium bicarbonate water (HCO_3–Ca), consists of six samples (Cacalotenango, Ejido Arroyo 1 and 2, Atzala, Hueymatla, Huamuchilito); this group was mostly found in springwater emanating from sedimentary rocks (Balsas, Mexcala, and Morelos Formations).

3.2. Water Quality of the Springwater

The quality of the springwater was evaluated according to the Mexican regulations, and the criteria of the World Health Organization, major elements, and trace elements (metals and metalloids) were assessed. The analysis was carried out by water group (Table 1). The HCO_3–Na water group does not present any of the physicochemical parameters outside the limits recommended by the quality criteria of both regulations. Only the Mulata spring presented nitrates above the limit of the Mexican standard. The presence of iron, fluorine, and barium was detected in almost all the samples of the group, but all of them were below the national and international limits; only the Cascada spring exceeds the criteria of the World Health Organization for iron.

For the HCO_3–Ca–SO_4–Mg group, as can be seen in Table 1, almost all the physicochemical parameters are within the recommended norms; the Landa, Ejido Arroyo 1 and Arroyo 1 springs slightly exceed the limit of the Mexican standard for nitrates. The presence of iron, fluorine, and barium was detected in almost all the samples of the group but within the national and international limits. The Pozitos spring exceeds the national and international manganese limits, while in the Pedro Martín spring, arsenic is above the criteria of the WHO standards.

Regarding the HCO_3–Ca group, the springs show some physicochemical parameters above the limits of the Mexican and WHO standards. The Taxco El Viejo 1 and 2 springs exceed the limit for total hardness; only Taxco El Viejo 2 is above the nitrate limit. The presence of iron, fluorine, and barium was detected in almost all the samples of the group within the national and international limits, and Table 1 shows the presence outside the limits of lead and iron in the Ejido Arroyo 2 spring and only iron in the Huamuchilito spring.

3.3. Chemical Composition of Springwater

The chemical composition of groundwater is the result of different factors, including infiltrating rainwater, geological structure, vadose zone characteristics, mineralogical composition of hosting rocks, and anthropogenic activities in the area. Correlations between dissolved species (major and minor anions and trace elements) can explain the process that generated the observed water compositions [12,41,42].

Bicarbonate ion (HCO_3^-) is the dominant anion in springwater of this area, as a product of rainwater plus carbon dioxide. Carbon dioxide originates from rainwater; its activity in the edaphic zone and the respiration of organic matter creates carbonic acid when it dissociates from hydrogen and carbonate ions. This process can be shown as follows:

$$H_2O + CO_2 \rightarrow H_2CO_3 \text{ and } H_2CO_3 \rightarrow H^+ + HCO_3^-, \quad (1)$$

Carbonate weathering involves the dissolution of calcite to produce calcium and bicarbonate ions in the reaction as follows:

$$CaCO_3 + H^+ + HCO_3 \rightarrow Ca^{2+} + 2\,HCO_3^- \quad (2)$$

The weathering of plagioclase as albite is a process that leads to the enrichment of Na+ in springwater [41–44]. To assess the role of the dissolution mechanisms of carbonate compounds (including the effect of CO_2) and the role of alteration of plagioclase in the samples, a $Ca^{2+} + Mg^{2+}$ vs. HCO_3^-- scatter diagram was created (Figure 4a). It may be observed that the points Horconcito 1 and 2, Cascada, Huamuchilito, Chacoalco, Mulata, Landa, and Cacalotenngo are located above y = x, indicating that carbonate weathering is the dominant process for the supply of the calcium ions to this springwater and a reduction in cations due to ionic exchange. In Figure 4b, the relationship of HCO_3^- to $Na^+ + K^+$ is shown to verify the alteration of plagioclase and carbonates [43]. In this figure, the observation points tend to fall above y = 2x, indicating a process of plagioclase alteration in the springs that emerge in the volcanic rocks of Tilzapotla Formation (group 1).

Albite weathering and rainwater is the reason for the presence of sodium in the springwater. However, samples with a Na/Cl ratio around or less than one indicate the possibility of some other chemical processes, such as ion exchange (Figure 4c). These proportions of cationic content could indicate water–rock interactions [42].

On the other hand, the increase in HCO_3^- concentration compared to Na^+ concentration in the springwater indicates the dominancy of the carbonate weathering process in the lower parts of the area Pozitos, Chacoalco, Pedro Martín, Cacalotenango, Ejido Arroyo 1 and 2, Atzala, Hueymantla, and Huamuchilito Taxco El Viejo 1 and 2. The ferromagnesian silicates weathering is a process that helps to produce Fe and Mg in the springwater. The main factors controlling the presence of Mg and Fe in springwater are pH, redox conditions, and the presence of organic or inorganic ligands [41].

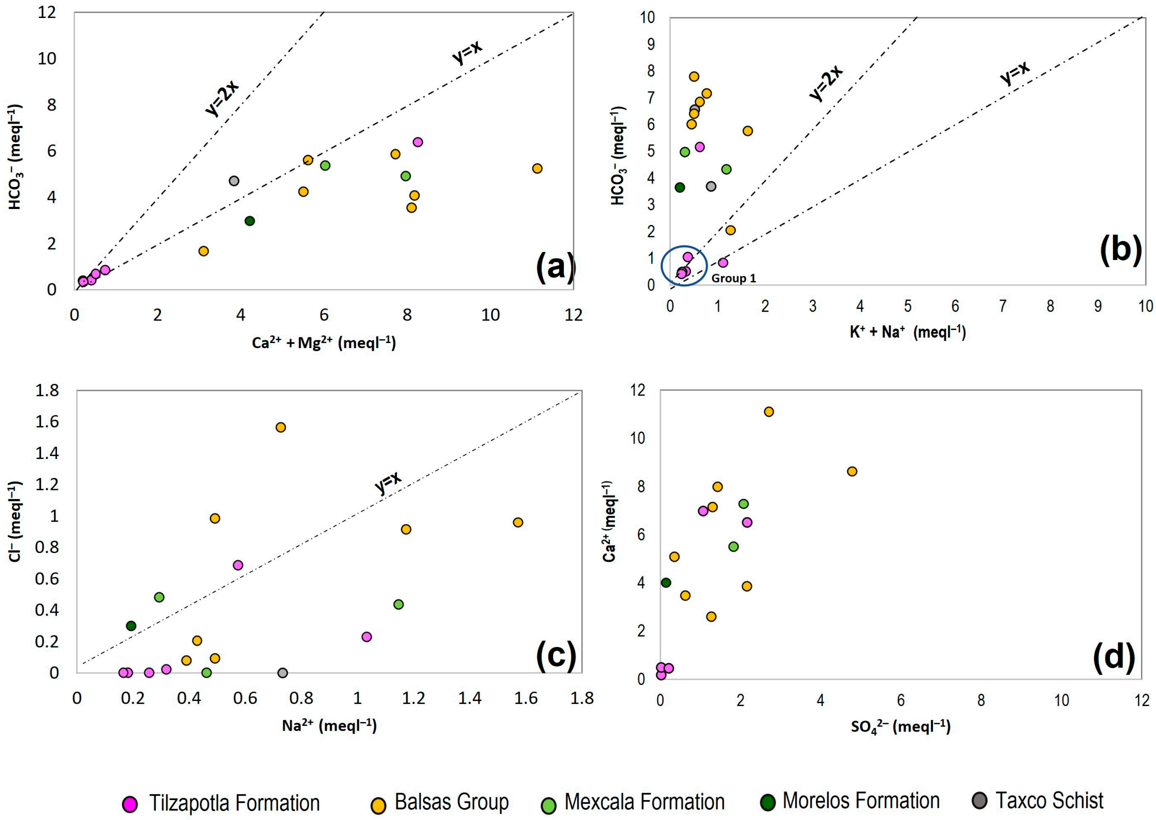

Figure 4. Plots of scattergrams (**a**) Ca^{2+} + Mg^{2+} vs. HCO_3^- + SO_4^{2-}, (**b**) Na^+ + K vs. HCO_3^- (**c**) Cl^- vs. Na+, (**d**) Ca^{2+} vs. SO_4^{2-}.

There are various sources of sulfates in the springwater that including atmospheric deposition, mineral dissolution, and anthropogenic sources as lixiviation of mining tailings.

3.4. Environmental Isotopes

3.4.1. Deuterium and Oxygen Isotopes and Recharge Altitudes

The isotopic values ranged from −8.28 ‰ to −11.6‰ for δ^{18}O and −61.6‰ to −75.4‰ for δ^2H in the present study. These samples and data from Talavera et al. [21] were plotted (Table 2 and Figure 5) along the Global Meteoric Water Line (GMWL), $\delta^2H = 8\ \delta^{18}O + 10$ [45], the Local Meteoric Water Line (LMWL) for the Mexico central region, $\delta^2H = 7.95\ \delta^{18}O + 11.7$ [46], and the Evaporation Line using surface water of the Taxco region for the dry season reported by Dótor et al. [25]; $\delta^2H = 3.99\ \delta^{18}O - 29.02$.

The springs had isotopic compositions close to the Global Meteoric Water Line (GMWL) and the Local Meteoric Water Line (LMWL); this springwater has a similar composition to rainwater, as reported by Talavera et al. [21] for the springwater in the region. The Hueymatla sample is more significantly displaced to the right from the GMWL, suggesting a higher degree of evaporation (slightly fractionated water), like those reported in 2016 [21] for the springwater from Estacas, La Bomba, and Copal, which have heavier isotopic compositions (Figure 5).

Determining the altitudes and recharge areas of sources is essential for the management of groundwater resources. The distribution of hydrogen and oxygen isotopic composition in groundwater samples, shown in Figure 5, provides an initial understanding of the origin of groundwater in the region. Table 2 gives the values of δ^{18}O and the altitudes of the different groundwater production sites.

The isotopic analysis indicates that the Horconcito, Equipada, Chacualco, Molanca, and Agua Zarca springs were recharged at a higher altitude than the rest of the saImples around 2000 to 2700 masl, which is the highest altitude of the mountain range in the area (capture zone) because they are isotopically heavier than Hueymatla, La Bomba, and Copal springs located at lower altitudes. The estimation of the recharge altitude indicates that the most important area within the region is the Huizteco hill, which is the main recharge area of the studied springs.

Table 2. Composition of the oxygen isotopes and recharge altitude.

	δ^{18} O (‰)	δ^{2}H (‰)	Recharge Altitude
Springwater			
Horconcito 1	−11.06	−75.4	2761.9
Mulata	−10.17	−71.1	2126.2
Landa	−9.86	−68.7	1904.8
Pedro Martin	–	–	1861.9
Arroyo 1	−9.35	−65.2	1540.5
Hueymatla	−8.28	−61.6	776.2
Chacualco [a]	−10.7	−77	2504.8
Estacas [a]	−9.3	−70	1504.8
La Molanca [a]	−10.6	−76	2433.4
Equipada [a]	−10.8	−78	2576.2
El Copal [a]	−8.5	−64	933.4
La Bomba [a]	−8.6	−66	1004.8
El Jumil [a]	−10.0	−73	2004.8
Pedro Martin [a]	−9.8	−71	
Agua Zarca [a]	−10.5	−75	2361.9
Rainwater			
Atzala [a]	−9.9	−71	
Minas Viejas [a]	−10.6	−75	
Taxco el Viejo [a]	−10.2	−73	
Taxco [a]	−10.4	−72	

Note(s): [a] Data from Talavera et al. [21].

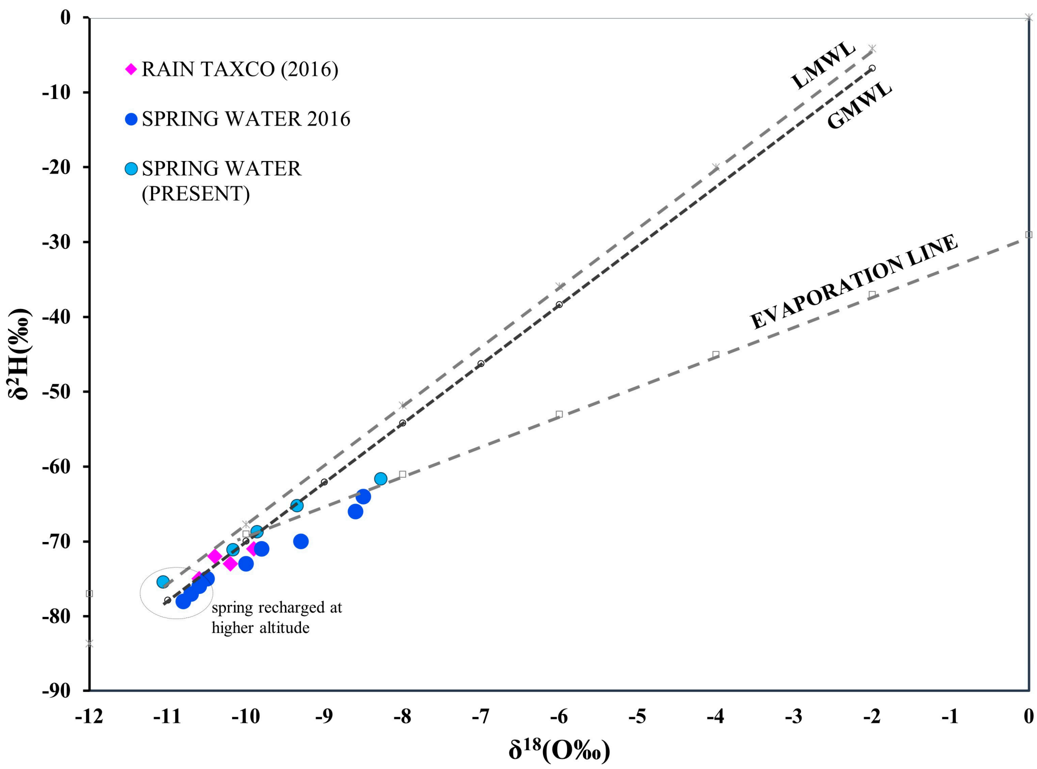

Figure 5. Relationships between δ^{2}H and δ^{18}O values. GMWL refers to Global Meteoric Water Line of Craig [45]. LMWL (local meteoric water line) for Mexico City [46] and Evaporation Line for the region [25].

3.4.2. Tritium Isotopes

The ^3H values range from 0.00 to 2.49 TU. The values in Table 2 show different processes and ages of the springwater. The first group with old water recharged prior to 1952 in Huamuchilito, Ejido Arroyo 2 and Hueymantla springs, has a low tritium content of less than 0.62 TU, representing a relatively long residence time and long interaction with rocks. Another group has at least 14 years since they were recharged, comprising sites such as Taxco el Viejo 1, Pedro Martín, and Pozitos, with tritium content from 1.10 to 1.13 TU, indicating modern water with intermediate circulation and residence time. The last group of younger water with tritium concentration from 1.42 to 2.49 TU, integrated by Horconcito 1, Mulata, Landa and Arroyo 1, Taxco el Viejo 2, indicates that these waters were recently recharged by local rainfall and rapid circulation.

Considering the equation of half-life of the tritium and its maximum reference value in the rainwater reported, the age of the groundwater was estimated. In this case, the measurements made in the springs of the area gave the estimated age of the recharge, showing the youngest and fast-flowing springs between 5 and 7 years, the intermediate flow springs of 14 years, and the oldest one between 25 and 27 years. Horst et al. [47] and Mahlknecht et al. [48] estimated the local input function of tritium in the Southwestern area of Mexico, using the International Atomic Energy Agency/Global Network of Isotope in Precipitation data from stations in Mexico. The activity of ^3H in rainwater in Central Mexico has been decreasing since the 1960s and finally dropped below 3 TU in 2007; it is estimated that the current tritium level has since stabilized between 2 and 3 TU.

3.4.3. Strontium Isotopes

The strontium isotopic ratios of the springwater obtained in the present study were compared to the isotopic ratios of the rocks of the five outcropping lithologies (schist, limestone, sandstone, siltstone, and rhyolite) reported by Talavera et al. [21]. The rocks reported have a variable Sr isotopic ratio composition that ranges from 0.70533 to 0.71528; volcanic rocks of the Tilzapotla Formation have the less radiogenic composition (0.70533), while the Taxco Schist has the most radiogenic composition (0.71528). The rocks of the Balsas Group have an isotopic composition of 0.70692, whereas Morelos Formation and the Mexcala Formation have values of 0.70746 and 0.70726, respectively (Table 3).

The springwater samples were grouped according to the $^{87}Sr/^{86}Sr$ isotopic ratio corresponding to each of the lithological formations in the study area. The first group, HCO3-Na water, corresponds to short-circulation springs that emerge in higher-altitude areas (between 2000 and 2700 m above sea level) in volcanic rocks, showing the weathering of sodium feldspars with an $^{87}Sr/^{86}Sr$ isotopic ratio that oscillates between 0.7057 and 0.7062, very similar to the measurement in the Tilzapotla Fm, so it can be inferred that the water only interacts with rocks of this formation (Table 3 and Figure 6).

The second group of springs is HCO_3-Ca-SO_4-Mg water that outcrops in conglomerates, breccias, and siltstones of the Balsas Group, showing slightly more radiogenic strontium values between the values of the Tilzapotla and Balsas Formations, and therefore the influence of the passage through both formations (Figure 6). The following HCO_3-Ca-type water group superimposes those of rocks belonging to the Balsas and Mexcala formations, registering a similar composition range (Table 3 and Figure 5). Only one sample from this group presented the most radiogenic $^{87}Sr/^{86}Sr$ ratio, indicating the influence of the metamorphic rocks of the Taxco Schist Fm, which represents the oldest lithology and the longest residence time according to the measured tritium value. In these two groups, the influence of sulfide minerals from hydrothermal veins as a product of mineralization can be glimpsed.

Table 3. Lithological, geochemical, and isotopic data (q.l. quantification limit).

Geological Formation	Lithology [a]	Rock $^{86}Sr/^{87}Sr$	Spring	Water Type	^{3}H (TU)	Sr (mgL^{-1})	Water $^{86}Sr/^{87}Sr$	Signature	Emerge
Tilzapotla Formation	Ignimbrites, vitrofides, and volcanic rocks (rhyolites)	0.70533	Horconcito 1	HCO_3-Na	2.49	0.028	0.70601	Tilzapotla	Tilzapotla
			Horconcito 2	HCO_3-Na	-	0.028	0.70619	Tilzapotla	Tilzapotla
			Cascada	HCO_3-Na	-	<ql.	0.7062	Tilzapotla	Tilzapotla
			Chacualco [b]	HCO_3-Na	-	0.022	0.70594 [b]	Tilzapotla	Tilzapotla
			Mulata	HCO_3-Na	1.42	0.043	0.70591	Tilzapotla	Tilzapotla
			Pozitos	HCO_3-Ca-SO_4-Mg	1.1	0.2	0.70572	Tilzapotla	Balsas
Balsas Group	Conglomerates, breccias, and siltstones	0.70692	Landa	HCO_3-Ca-SO_4-Mg	1.83	0.44	0.7066 [b]	Balsas	Balsas
			Pedro Martin	HCO_3-Ca-SO_4-Mg	1.13	0.3	0.70682	Balsas	Balsas
			Cacalotenango	HCO_3-Ca	-	0.41	0.70622	Balsas	Balsas
			Ejido de Arroyo 2	HCO_3-Ca	0.56	0.467	0.70708	Balsas	Mexcala
			Taxco el Viejo 1	HCO_3-Ca-SO_4-Mg	1.1	0.603	0.70658	Balsas	Mexcala
			Taxco el Viejo 2	HCO_3-Ca-SO_4-Mg	1.69	0.431	0.70705	Balsas	Mexcala
Mexcala	Sandstones, shales, marls, and limestones	0.70726	Arroyo 1	HCO_3-Ca-SO_4-Mg	2.49	0.414	0.70714	Mexcala	Mexcala
			Arroyo 2	HCO_3-Ca-SO_4-Mg	-	0.333	0.70714	Mexcala	Mexcala
Morelos	Reef and sub-reef limestones, dolomites, loams, and flint	0.70746	Atzala	HCO_3-Ca	-	0.146	0.70709	Morelos	Morelos
Taxco Schist	Milonites, sericite schists, meta-andesite, meta-rhyolite, quartzite	0.71528	Huamuchilito	HCO_3-Ca	0	0.096	0.70848	E. Taxco	E. Taxco

Note(s): [a] Data from Talavera et al. [21]. [b] Data from Arroyo et al. [49].

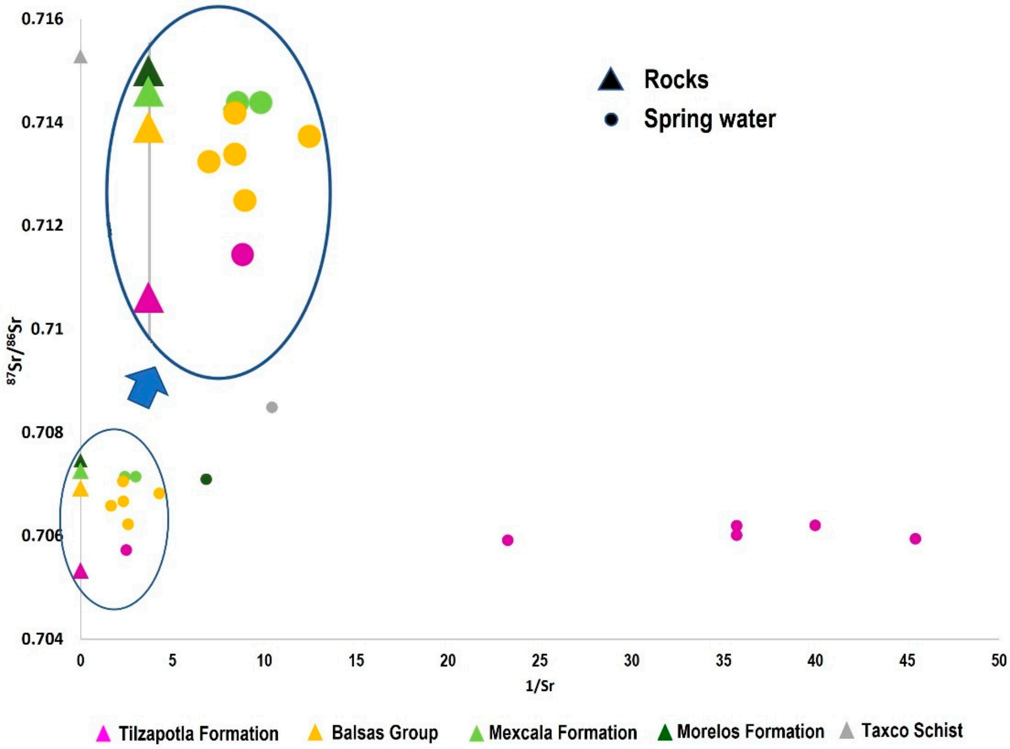

Figure 6. Plot of $^{87}Sr/^{86}Sr$ vs. 1/Sr.

Sr and Ca can be used to identify water–rock interaction processes and to define flow pathway systems, mainly by assessing dissolved Sr [48]. When the Sr concentrations in silicates are relatively lower than in carbonates, the dissolution of the silicates generates a low Sr concentration in the springwater [50]. In the area, there are no carbonate outcrops, but there are outcrops of volcanic rocks [50]. This type of lithology indicates that the release of Ca and Sr in springwater depends on processes related to mineral alteration of silicates (Figure 7). Therefore, the composition of the Sr isotope, which can be explained by the fact that the springwater only interacts with the rocks of the Tilzapotla Formation and the rocks are acting as important contributors of Sr. This ratio indicates that Ca and Sr have the same origin and are related to plagioclase in Tilzapotla and limestone horizons in Balsas.

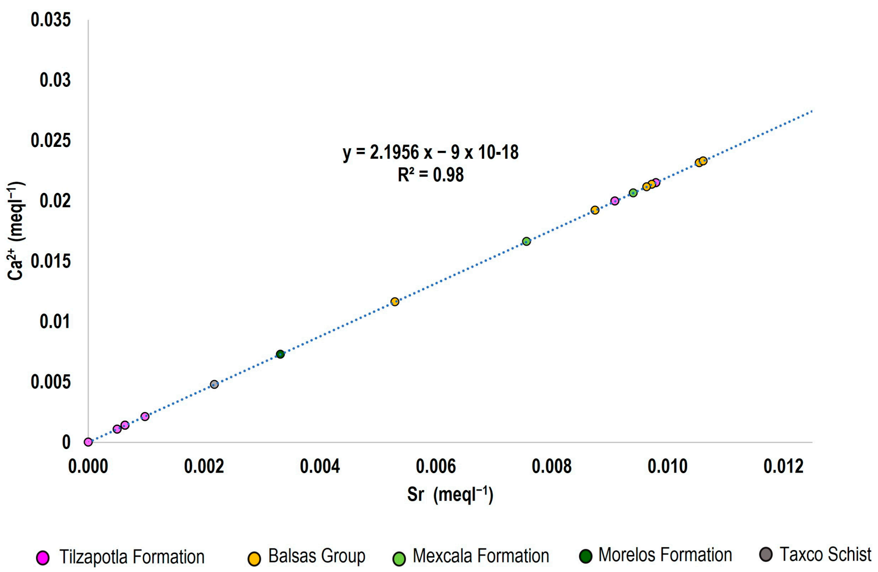

Figure 7. Ca vs. Sr diagram.

4. Conclusions

The chemical composition of springwaters can be grouped into three types of water. The springwater chemistry is mainly related to water–rock interaction processes.

The results of major ions and the trace metal concentrations indicated that the chemistry in the springwater samples was mainly the consequence of atmospheric deposition, rock dissolution, and anthropogenic contributions.

The mineralized structures in the area and the tailings do not have a clear influence on the quality of the springwater. The isotopic techniques and the hydrogeochemical analysis of this research lead to a chemical framework of the springwater that does not present a negative impact due to mining activity in the region. Moreover, the data confirm that the water comes from relatively recent infiltrated rainwater flowing through faults and fractures of different host rocks.

$\delta^{18}O$ and $\delta^{2}H$ indicate that the springwater comes from the meteoric water suffering some degree of isotopic fractionation by atmospheric evaporation, and the recharge altitude indicated that the Huizteco hill is an important recharge zone within the study area.

The tritium values confirm the short residence times of the springwater, which indicate the isotopic relationship of $^{87}Sr/^{86}Sr$; only a sample housed in the Taxco Schist presents a longer residence time according to this isotope.

The data indicated that springwater suffers important water–rock interactions. Strontium isotope ratios indicated the importance of volcanic rocks from the Tilzapotla formation as contributors to the springwater chemistry.

The results of this study show the utility of $^{87}Sr/^{86}Sr$ ratios in identifying the water–rock interactions and springwater flow paths, suggesting that more widespread use of the strontium isotopic fingerprint is warranted. The impact of groundwater–rock interaction depends mainly on the type of rocks and the residence time of groundwater.

Since the regional groundwater aquifer is very deep in the recharge area of Taxco; there is the possibility of the development of perched aquifers, such that once the groundwater is stored at different depths, it can feed some of the springs year-long, making this type of analysis very useful for regions with intermountain springs. The local authorities with this valuable information about hydrogeological and hydrochemical processes can implement protection measures on regional springs.

For future investigations, it is recommended to include a broader area to be able to identify the capture zone and the seasonal variability of the springs. The results of this study show the utility of $^{87}Sr/^{86}Sr$ ratios in identifying the water–rock interactions and springwater flow paths, suggesting that more widespread use of the strontium isotopic fingerprint is warranted. The impact of groundwater–rock interaction depends mainly on the types of rocks and the residence time of groundwater.

Author Contributions: J.A.F.R., Sampling collection and laboratory and data analysis; E.R.S.S., Sampling collection, data analysis, hydrogeochemical assessment, and paper writing and editing; M.M.M., Hydrogeological and isotopic assessment and analysis, paper editing; J.M.E.M., sampling collection, map editing, writing, and paper editing; M.V.E.A., Geochemical data analysis, paper writing, and editing; O.T.M., Isotopic analysis and paper editing. All authors have read and agreed to the published version of the manuscript.

Funding: This research received no external funding.

Data Availability Statement: The data of the chemical and isotope analyzes have been included in the present work.

Acknowledgments: We thank the support of Arizona University for the strontium isotopic analysis. We thank Sergio Salgado Souto for the laboratory support at Arizona University.

Conflicts of Interest: The authors do not have conflict of interest to declare.

References

1. Chen, D.; Feng, Q.; Gong, M. Contamination Characteristics and Source Identification of Groundwater in Xishan Coal Mining Area of Taiyuan Based on Hydrochemistry and Sulfur–Oxygen Isotopes. *Water* **2023**, *15*, 1169. [CrossRef]
2. Doveri, M.; Natali, S.; Franceschi, L.; Menichini, M.; Trifiró, S.; Giannecchini, R. Carbonate aquifers threatened by legacy mining: Hydrodynamics, hydrochemistry, and water isotopes integrated approach for spring water management. *J. Hydrol.* **2021**, *593*, 125850. [CrossRef]
3. Zamora, H.A.; Eastoe, C.J.; Wilder, B.T.; McIntosh, J.C.; Meixner, T.; Flessa, K.W. Groundwater Isotopes in the Sonoyta River Watershed, USA-Mexico: Implications for Recharge Sources and Management of the Quitobaquito Springs. *Water* **2020**, *12*, 3307. [CrossRef]
4. Pantoja-Irys, J.R.; Mujica-Sánchez, H.; Arista-Cázares, L.E.; Hernández-García, C.M.; Wagner, M. Environmental geology, and isotopic evaluation of springs within the central part of the Sierra Cerro de La Silla, northeastern México. *J. S. Am. Earth Sci.* **2022**, *119*, 104017. [CrossRef]
5. Khayat, S.; Marei, A.; Hippler, D.; Barghouthi, Z.; Dietzel, M. Using environmental isotopes to investigate the groundwater recharge mechanisms and dynamics in the North-eastern Basin, Palestine. *Hydrol. Sci. J.* **2020**, *65*, 583–596. [CrossRef]
6. Madrigal-Solís, H.; Jiménez-Gavilán, P.; Vadillo-Pérez, I.; Fonseca-Sánchez, A.; Quesada-Hernández, L.; Sánchez-Gutiérrez, R.; Calderón-Sánchez, H.; Pardo-Vargas, C. Application of hydrogeochemistry and isotopic characterization for the assessment of recharge in a volcanic aquifer in the eastern region of central Costa Rica. *Isot. Environ. Health Stud.* **2021**, *56*, 446–464. [CrossRef]
7. López, S.; Expósito, J.L.; Esteller, M.V.; Gómez, M.A.; Franco, R.; Morales, G.P. Prioritization to protect springs for public urban water supplies, based on multi-criteria evaluation and GIS (State of Mexico, Mexico). *Appl. Geogr.* **2019**, *107*, 26–37. [CrossRef]
8. Ranjan, P.; Pandey, P.K. Spring Protection: Step Towards Water Security and Sustainable Rural Water Supply. *Ann. Rom. Soc. Cell Biol.* **2021**, *25*, 1216–1222.
9. Zhou, J.; Zhang, Y.; Zhang, Q.; Kang, F.; Yuan, L.; Wei, D.; Lin, S. Using multi-isotopes (^{34}S, ^{18}O, ^{2}H) to track local contamination of the groundwater from Hongshan-Zhaili abandoned coal mine, Zibo city, Shandong Province. *Int. Biodeterior. Biodegrad.* **2018**, *128*, 48–55. [CrossRef]
10. Page, D.; Bekele, E.; Vanderzalm, J.; Sidhu, J. Managed Aquifer Recharge (MAR) in Sustainable Urban Water Management. *Water* **2018**, *10*, 239. [CrossRef]
11. Qu, S.; Wang, G.; Shi, Z.; Xu, Q.; Guo, Y.; Ma, L.; Sheng, Y. Using stable isotopes (δD, δ ^{18}O, δ ^{34}S and ^{87}Sr/^{86}Sr) to identify sources of water in abandoned mines in the Feng coal mining district, Northern China. *Hydrogeol. J.* **2018**, *26*, 1443–1453. [CrossRef]
12. Barbieri, M.; Morotti, M. Hydrogeochemistry and strontium isotopes of spring and mineral waters from monte Vulture Volcano, Italy. *Appl. Geochem.* **2003**, *18*, 117–125. [CrossRef]
13. Anuard, P.-G.; Julián, G.-T.; Hugo, J.-F.; Carlos, B.-C.; Arturo, H.-A.; Edith, O.-T.; Claudia, Á.-S. Integration of Isotopic (^{2}H and ^{18}O) and Geophysical Applications to Define a Groundwater Conceptual Model in Semiarid Regions. *Water* **2019**, *11*, 488. [CrossRef]
14. Tian, X.; Gong, Z.; Fu, L.; You, D.; Li, F.; Wang, Y.; Chen, Z.; Zhou, Y. Determination of Groundwater Recharge Mechanism Based on Environmental Isotopes in Chahannur Basin. *Water* **2023**, *15*, 180. [CrossRef]
15. Xiao, L.; Xu, Y.; Talma, A.S. Hydrochemical and isotopic approach to dynamic recharge of a dolomite aquifer in South Africa. *Hydrogeol. J.* **2019**, *27*, 945–964. [CrossRef]
16. Nigro, A.; Sappa, G.; Barbieri, M. Strontium Isotope as Tracers of Groundwater Contamination. *Procedia Earth Planet. Sci.* **2017**, *17*, 352–355. [CrossRef]
17. Stewart, M.K.; Taylor, C.B. Environmental isotopes in New Zealand hydrology. 1. Introduction. The role of oxygen-18, deuterium, and tritium in hydrology. *N. Z. J. Sci.* **1981**, *24*, 295–311.
18. Ayadi, R.; Trabelsi, R.; Zouari, K.; Saibi, H.; Itoi, R.; Khanfir, H. Hydrogeological and hydrochemical investigation of groundwater using environmental isotopes (^{18}O, ^{2}H, ^{3}H, ^{14}C) and chemical tracers: A case study of the intermediate aquifer, Sfax, Southeastern Tunisia. *Hydrogeol. J.* **2018**, *26*, 983–1007. [CrossRef]
19. Moya, C.; Raiber, M.; Taulis, M.; Cox, M. Using environmental isotopes and dissolved methane concentrations to constrain hydrochemical processes and inter-aquifer mixing in the galilee and eromanga basins, great artesian basin, Australia. *J. Hydrol.* **2016**, *539*, 304–318. [CrossRef]
20. Salcedo Sánchez, E.R.; Martínez, J.M.E.; Morales, M.M.; Talavera Mendoza, O.; Alberich, M.V.E. Ecological and Health Risk Assessment of Potential Toxic Elements from a Mining Area (Water and Sediments): The San Juan-Taxco River System, Guerrero, Mexico. *Water* **2022**, *14*, 518. [CrossRef]
21. Talavera, M.O.; Ruiz, J.; Díaz, V.E.; Ramírez, G.A.; Cortés, A.; Salgado, S.S.A.; Rivera, B.R. Water-rock-tailings interactions and sources of sulfur and metals in the subtropical mining region of Taxco, Guerrero (Southern Mexico): A multi-isotopic approach. *Appl. Geochem.* **2016**, *66*, 73–81. [CrossRef]
22. DOF. *CONAGUA, Actualización de la Disponibilidad Media Anual de Agua en el Acuífero Buena vista de Cuellar (1204), Estado de Guerrero*; Comisión Nacional del Agua: Mexico City, México, 2015; Available online: https://www.gob.mx/cms/uploads/attachment/file/103667/DR_1204.pdf (accessed on 20 April 2015).

23. DOF. *CONAGUA Actualización de la Disponibilidad Media Anual de Agua en el Acuífero de Iguala (1205), Estado de Guerrero*; Comisión Nacional del Agua: Mexico City, México, 2015; Available online: https://www.gob.mx/cms/uploads/attachment/file/103668/DR_1205.pdf (accessed on 20 April 2015).
24. Dótor-Almazán, A.; Armienta-Hernández, M.A.; Talavera-Mendoza, O.; Ruiz, J. Geochemical behavior of cu and sulfur isotopes in the tropical mining region of Taxco, Guerrero (southern Mexico). *Chem. Geol.* **2017**, *471*, 1–12. [CrossRef]
25. Dotor, A.A.; Armienta, M.A.; Arcega, F.; Talavera, M.O. Procesos de transporte de arsénico y metales en aguas superficiales del distrito minero de Taxco, Mexico: Aplicación de isótopos estables (Transport processes of arsenic and metals in surface waters in the mining district of Taxco, Mexico). *Hidrobiológica* **2014**, *24*, 256.
26. Norwegian Meteorological Institute. 2019. Available online: http://www.weatherbase.com/weather/weather.php3?s=912122&cityname=Taxco%2C+Guerrero%2C+Mexico&units=&set=metric (accessed on 30 March 2023).
27. Armienta, M.A.; Talavera, O.; Villaseñor, G.; Espinosa, E.; Pérez-Martínez, I.; Cruz, O.; Ceniceros, N.; Aguayo, A. Environmental behaviour of metals from tailings in shallow rivers: Taxco, central Mexico. *Appl. Earth Sci.* **2004**, *113*, 76–82. [CrossRef]
28. Romero, F.M.; Núñez, L.; Gutiérrez, M.E.; Armienta, M.A.; Ceniceros-Gómez, A.E. Evaluation of the potential of indigenous calcareous shale for neutralization and removal of arsenic and heavy metals from acid mine drainage in the Taxco mining area, Mexico. *Arch. Environ. Contam. Toxicol.* **2011**, *60*, 191–203. [CrossRef]
29. Talavera, M.O.; Moreno, T.R.; Dotor-Almazán, A.; Flores-Mundo, N.; Duarte Gutiérrez, C. Mineralogy and geochemistry of sulfide-bearing tailings from silver mines in the Taxco, Mexico Area to evaluate their potential environmental impact. *Geofísica Int.* **2005**, *44*, 49–64. [CrossRef]
30. Ruiz, H.E.; Armienta, H.M.A. Acumulación de arsénico y metales pesados en maíz en suelos cercanos a jales o residuos mineros. Rev. *Int. Contam. Ambient* **2012**, *28*, 103–117.
31. Gómez, B.J.M.; Santana, C.J.; Romero, M.F.; Armienta, H.M.A.; Morton, B.O.; Ruiz, H.E.A. Plantas de sitios contaminados con desechos mineros en Taxco, Guerrero. *México. Bol. Soc. Bot. Mex.* **2010**, *87*, 131–133.
32. Vázquez, B.A.; Talavera, M.O.; Moreno, G.M.; Salgado, S.S.; Ruiz, J.; Huerta, B.G. Source apportionment of lead in the blood of women of reproductive age living near tailings in Taxco, Guerrero, Mexico: An isotopic study. *Sci. Total Environ.* **2017**, *583*, 104–114. [CrossRef]
33. Campa, U.M.F.; Ramírez, E.J. La evolución geológica y la metalogenesis del noroccidente de Guerrero (The Geological Evolution and Metallogeny of Northwest Guerrero). In *Serie Técnico-Científica*; Universidad Autónoma de Guerrero: Chilpancingo, Mexico, 1979; Volume 1, p. 101.
34. DOF. NOM-230-SSA1-2002, Salud Ambiental. Agua Para uso y Consumo Humano, Requisitos Sanitarios que se Deben Cumplir en los Sistemas de Abastecimiento Públicos y Privados Durante el Manejo del Agua. Procedimientos Sanitarios Para el Muestreo. Diario Oficial de la Federación (DOF). 4 November 2003. Available online: https://dof.gob.mx/nota_detalle.php?codigo=2081772&fecha=12/07/2005 (accessed on 30 March 2023).
35. APHA; AWWA; WEF. *Standard Methods for the Examination Water and Wastewater*, 21st ed.; APHA; AWWA; WEF: Washington, DC, USA, 2004.
36. Deutsch, W. *Groundwater Geochemistry. Fundamentals and Applications to Contamination*; Lewis Publishers: New York, NY, USA, 1997.
37. Thibodeau, A.M.; Habicht-Mauche, J.; Huntley, D.L.; Chesley, J.T.; Ruiz, J. High precision isotopic analyses of lead ores from New Mexico by MC-ICP-MS: Implications for tracing the production and exchange of Pueblo IV glaze-decorated pottery. *J. Archaeol. Sci.* **2013**, *40*, 3067–3075. [CrossRef]
38. WHO (World Health Organization). *Guidelines for Drinking-Water Quality [Electronic Resource]: Incorporating 1st and 2nd Addenda*, 3rd ed.; WHO: Geneva, Switzerland, 2008; Volume 1.
39. DOF. Norma Oficial Mexicana NOM-127-SSA1-2021 Agua Para uso y Consumo Humano. Límites Permisibles de la Calidad del Agua. Secretaria de Salud. Diario Oficial de la Federación (DOF). 5 May 2022. Available online: https://www.dof.gob.mx/nota_detalle.php?codigo=5650705&fecha=02/05/2022 (accessed on 30 March 2023).
40. Aqueous Solutions LCC. *Geochemist's Workbench*, Version 11; Department of Geology at the University of Illinois Urbana Champaign: Urbana, IL, USA, 2016. Available online: https://www.gwb.com/(accessed on 30 March 2023).
41. Appelo, C.; Postma, D. *Geochemistry, Groundwater and Pollution*, 2nd ed.; Routledge: New York, NY, USA, 2005.
42. Esteller, M.V.; Kondratenko, N.; Expósito, J.L.; Medina, M.; Martin del Campo, M.A. Hydrogeochemical characteristics of a volcanic-sedimentary aquifer with special emphasis on Fe and Mn content: A case study in Mexico. *J. Geochem. Explor.* **2017**, *180*, 113–126. [CrossRef]
43. Biswas, A.; Nath, B.; Bhattacharya, P.; Halder, D.; Kundu, A.K.; Mandal, U.; Mukherjee, A.; Chatterjee, D.; Mörth, C.M.; Jacks, G. Hydrogeochemical contrast between brown and grey sand aquifers in shallow depth of Bengal Basin: Consequences for sustainable drinking water supply. *Sci. Total Environ.* **2012**, *431*, 402–412. [CrossRef]
44. Zhang, B.; Zhao, D.; Zhou, P.; Qu, S.; Liao, F.; Wang, G. Hydrochemical Characteristics of Groundwater and Dominant Water–Rock Interactions in the Delingha Area, Qaidam Basin, Northwest China. *Water* **2020**, *12*, 836. [CrossRef]
45. Craig, H. Isotopic variations in meteoric waters. *Science* **1961**, *133*, 1702–1703. [CrossRef]
46. Cortes, A.; Farvolden, R.N. Isotope studies of precipitation and groundwater in the Sierra de las Cruces, Mexico. *J. Hydrol.* **1988**, *107*, 147–153. [CrossRef]

47. Horst, A.; Mahlknecht, J.; Merkel, B.J.; Aravena, R.; Ramos-Arroyo, Y.R. Evaluation of the recharge processes and impacts of irrigation on groundwater using CFCs and radiogenic isotopes in the Silao-Romita basin, Mexico. *Hydrogeol. J.* **2008**, *16*, 1601–1614. [CrossRef]
48. Mahlknecht, J.; Daessle, L.W.; Esteller, M.V.; Torres-Martinez, J.A.; Mora, A. Groundwater flow processes and human impact along the arid US-mexican border, evidenced by environmental tracers: The case of tecate, baja california. *Int. J. Environ. Res. Public Health* **2018**, *15*, 887. [CrossRef]
49. Arroyo-Díaz, F.; Salgado-Souto, S.A.; Del Rio-Salas, R.; Talavera-Mendoza, O.; Ramírez-Guzmán, A.; Ruíz, J.; Sarmiento-Villagrana, A.; Guzmán-Martínez, M. PTE and Multi-Isotope Assessment of Spring Water Used for Human Consumption in the Historical Mining Region of Taxco de Alarcón in Southern Mexico. *J. S. Am. Earth Sci.* **2022**, *116*, 103811. [CrossRef]
50. Morales-Arredondo, J.I.; Armienta Hernández, M.A.; Cuellar-Ramírez, E.; Morton-Bermea, O.; Ortega-Gutiérrez, J.E. Hydrogeochemical behavior of Ba, B, Rb, and Sr in an urban aquifer located in central Mexico and its environmental implications. *J. S. Am. Earth Sci.* **2022**, *116*, 103870. [CrossRef]